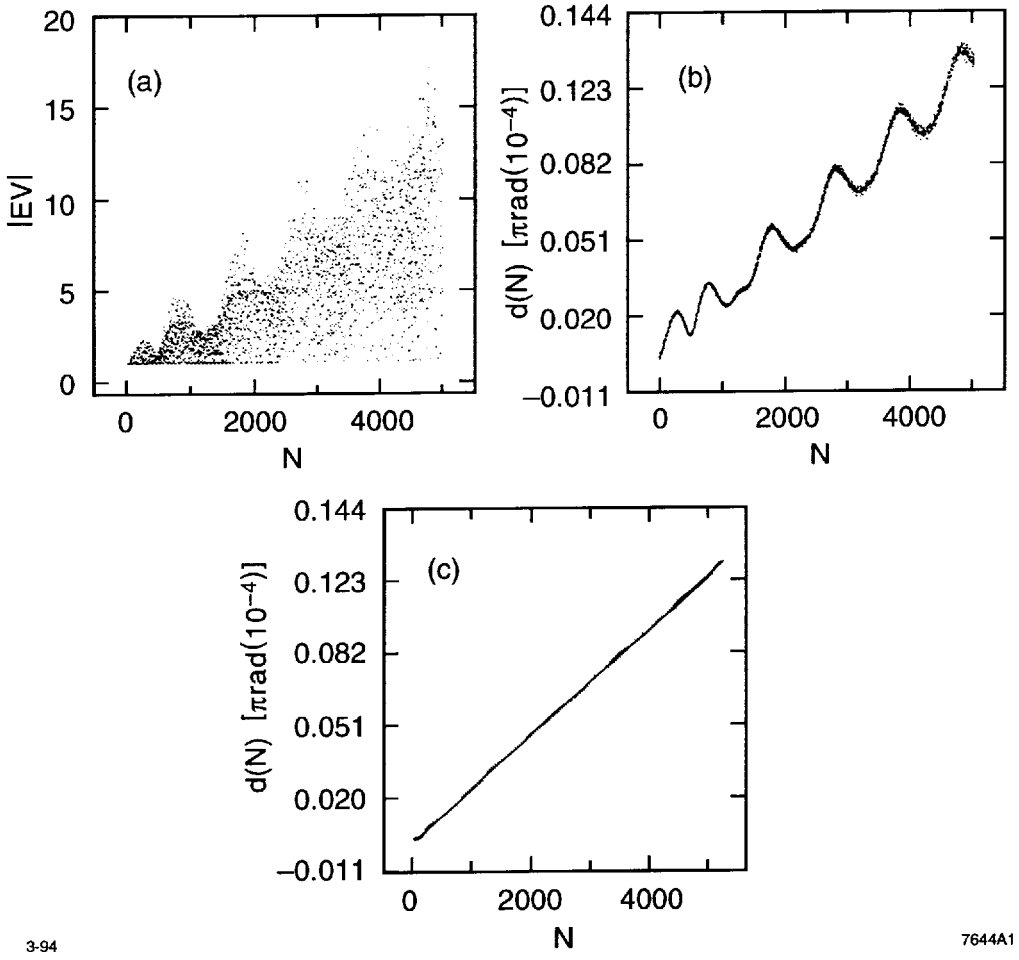

Figure 1:

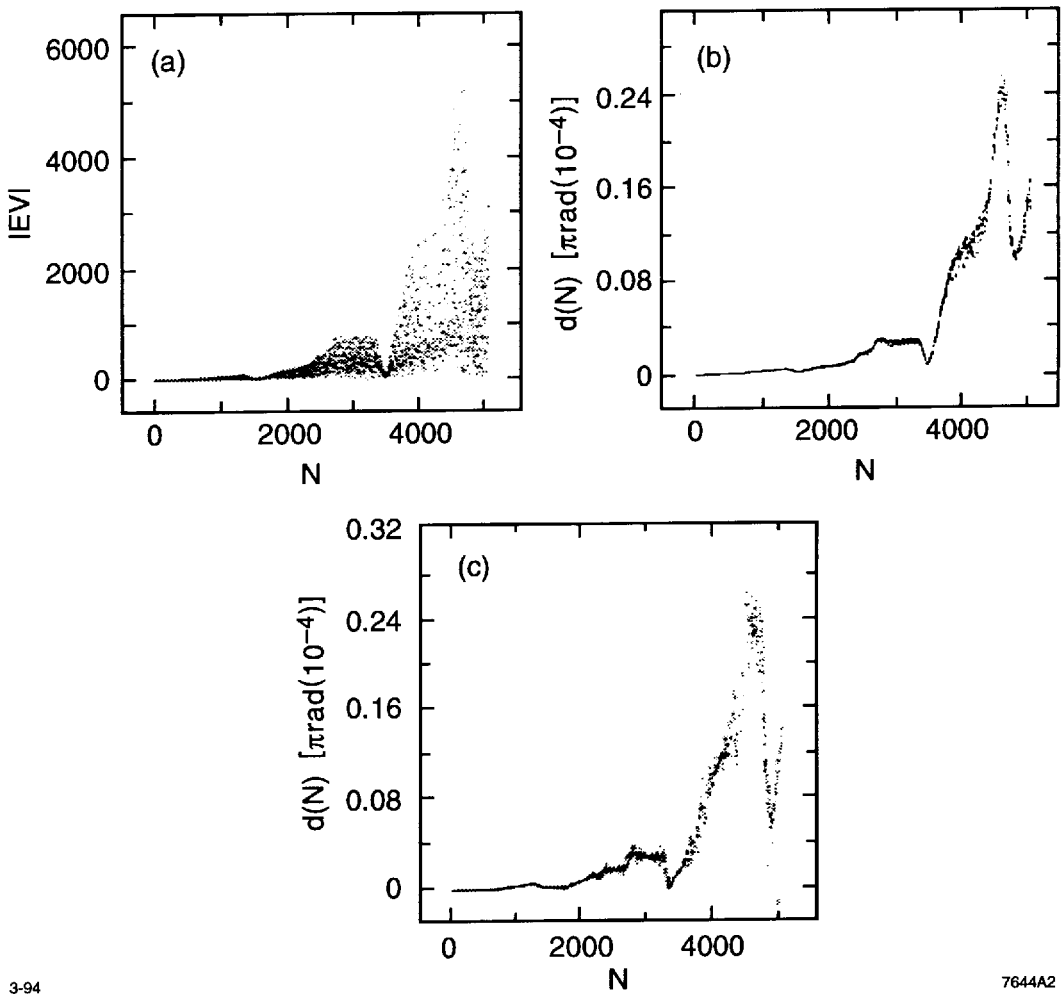
(a)
6000
4000
2000
0
|EV|
0
2000
4000
N
(b)
0.24
0.16
0.08
0
d(N) [πrad(10⁻⁴)]
0
2000
4000
N
(c)
0.32
0.24
0.16
0.08
0
d(N) [πrad(10⁻⁴)]
0
2000
4000
N
3-94
7644A2

Figure 2:

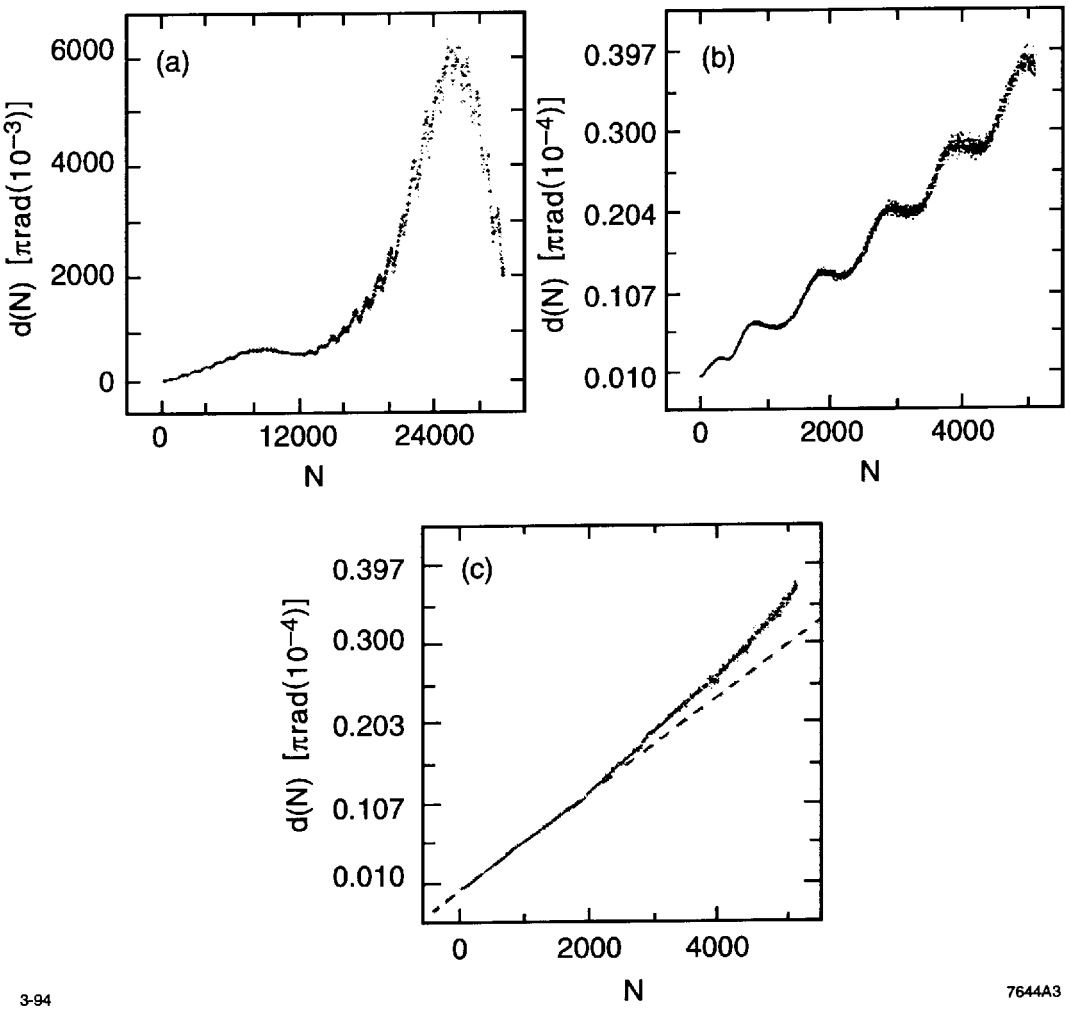
(a)
6000
4000
2000
0
d(N) [πrad(10⁻³)]
0
12000
24000
N
(b)
0.397
0.300
0.204
0.107
0.010
d(N) [πrad(10⁻⁴)]
0
2000
4000
N
(c)
0.397
0.300
0.203
0.107
0.010
d(N) [πrad(10⁻⁴)]
0
2000
4000
N
3-94
7644A3

Figure 3:

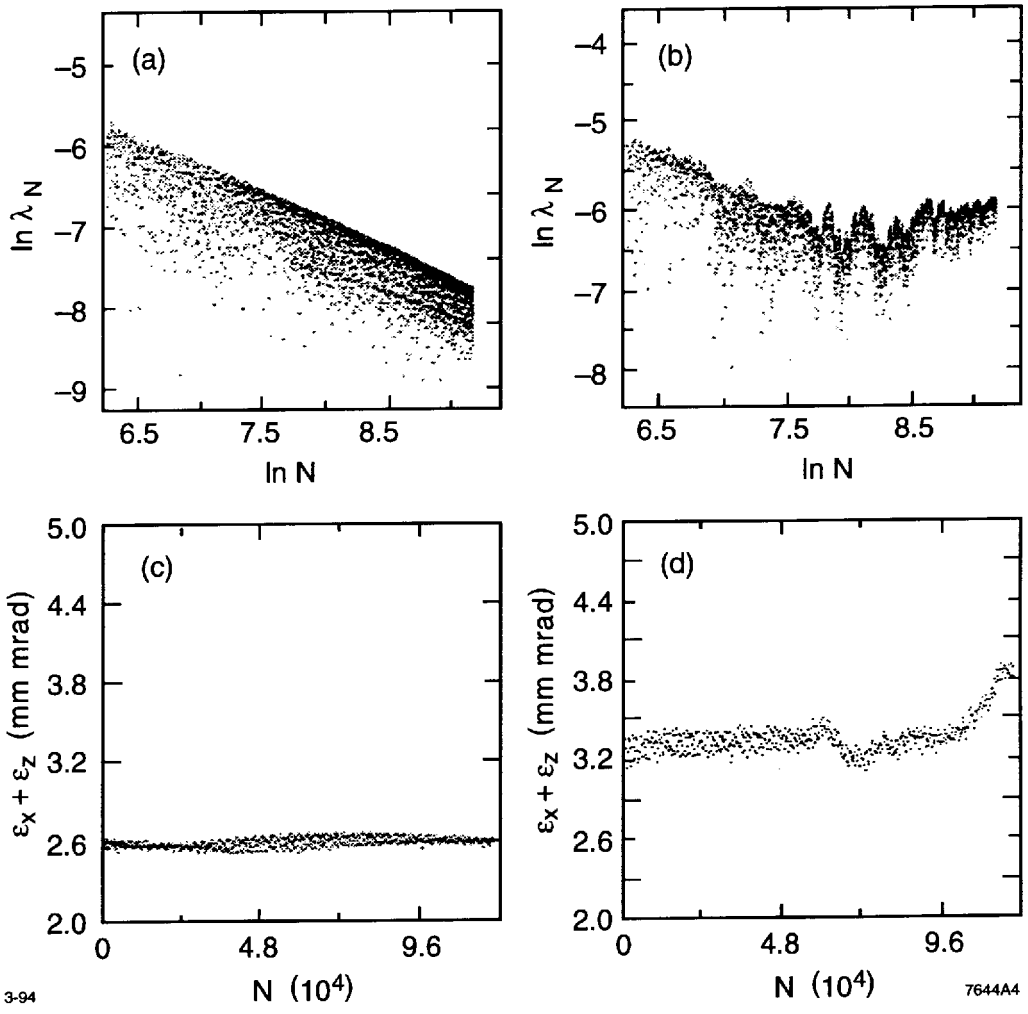

Figure 4:

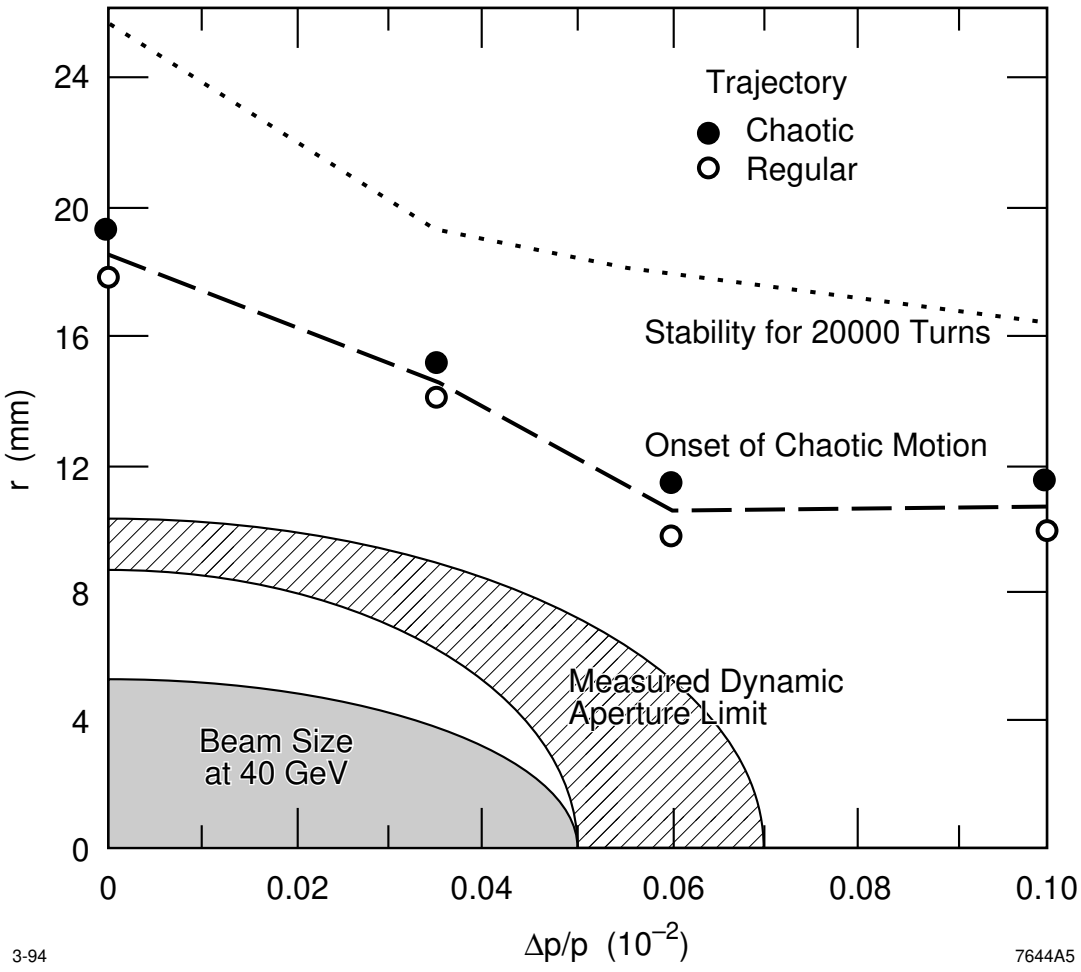
Trajectory
Chaotic
Regular
Stability for 20000 Turns
Onset of Chaotic Motion
Measured Dynamic
Aperture Limit
Beam Size
at 40 GeV
r (mm)
Δp/p (10^−2)
0
4
8
12
16
20
24
0
0.02
0.04
0.06
0.08
0.10
3-94
7644A5

Figure 5:

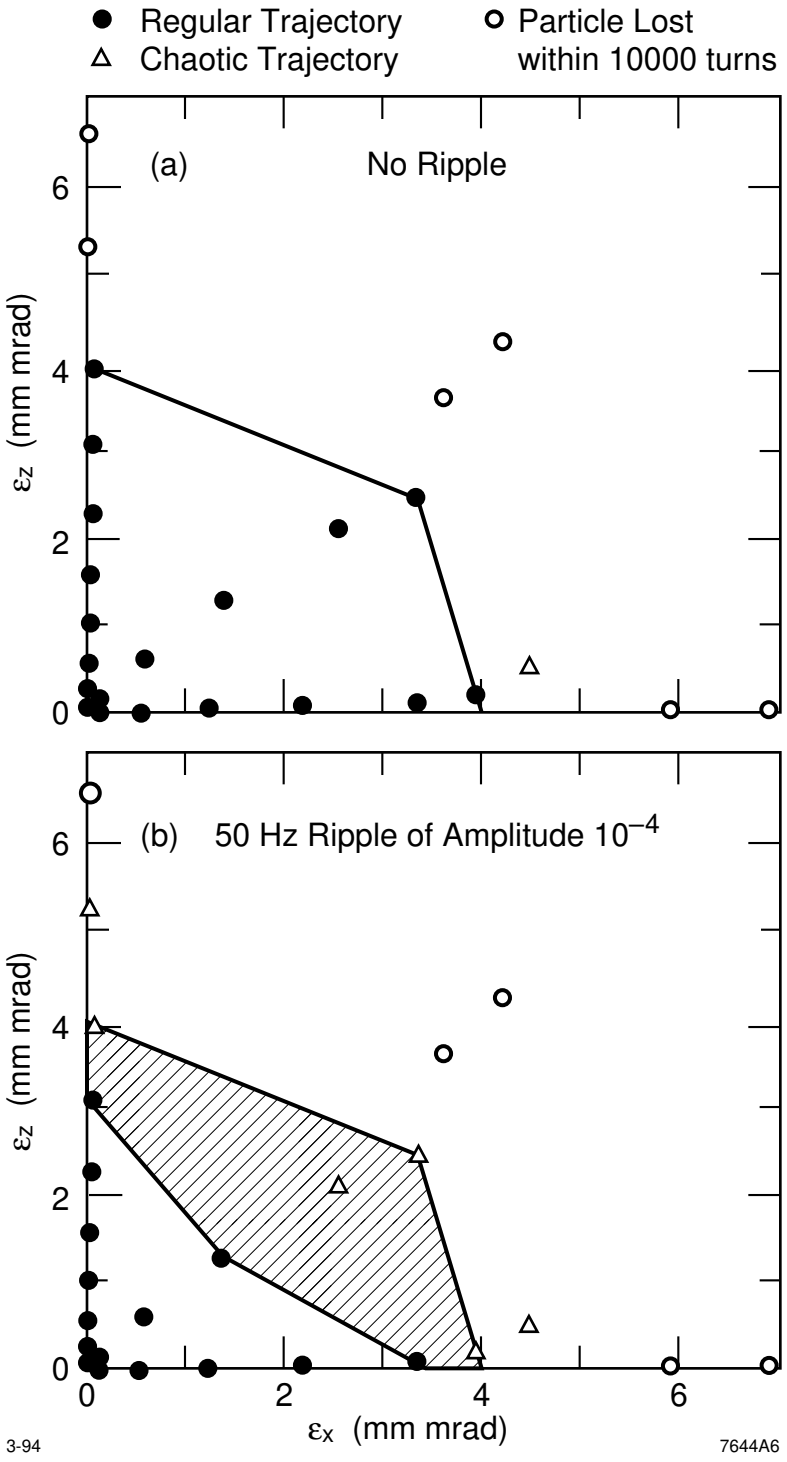
Regular Trajectory
Particle Lost
within 10000 turns
Chaotic Trajectory
(a) No Ripple
(b) 50 Hz Ripple of Amplitude 10^{-4}
ε_z (mm mrad)
ε_x (mm mrad)
0
2
4
6
3-94
7644A6

Figure 6:

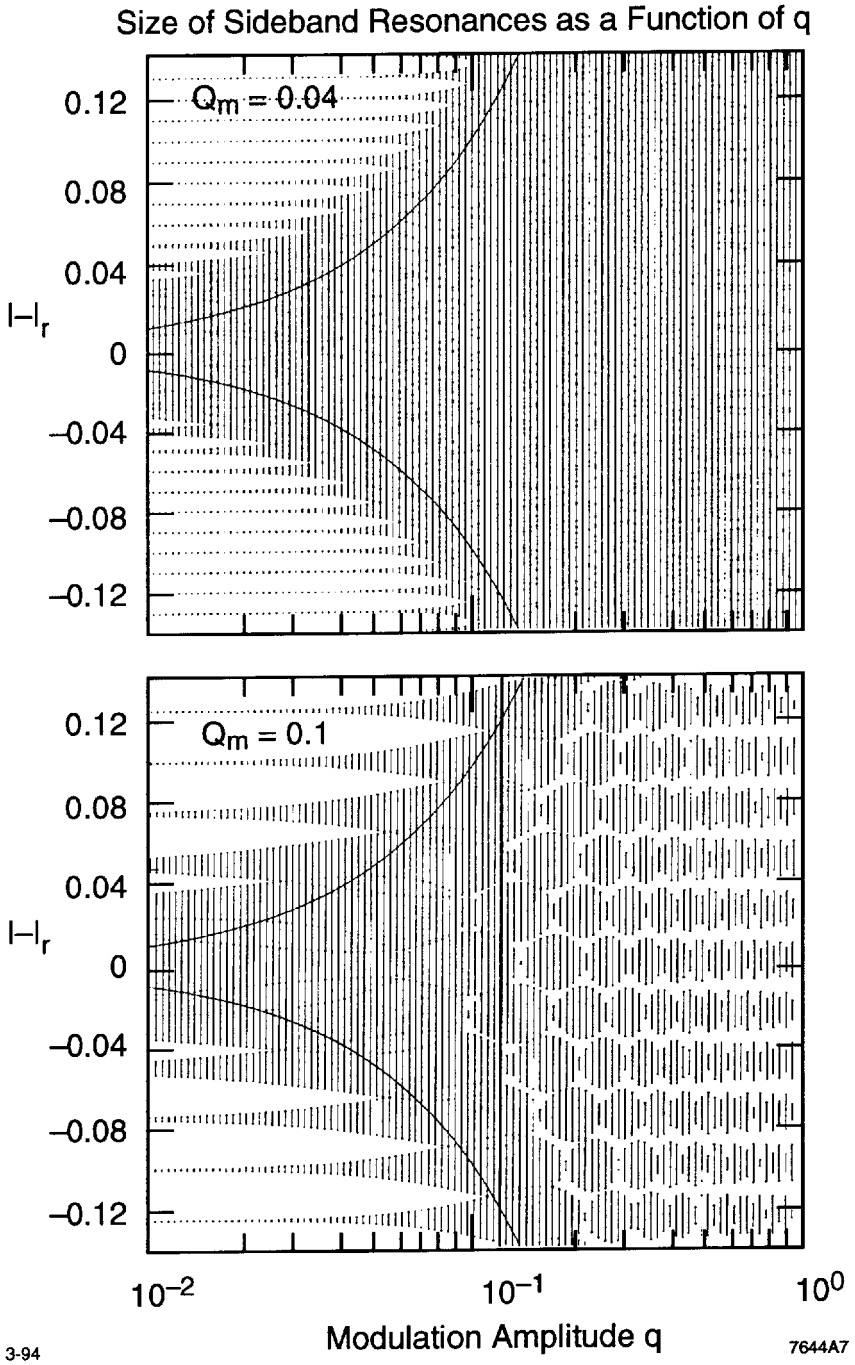
Size of Sideband Resonances as a Function of q
$Q_m = 0.04$
$Q_m = 0.1$
0.12
0.08
0.04
0
–0.04
–0.08
–0.12
$I-I_r$
10^{-2}
10^{-1}
10^{0}
Modulation Amplitude q
3-94
7644A7

Figure 7:

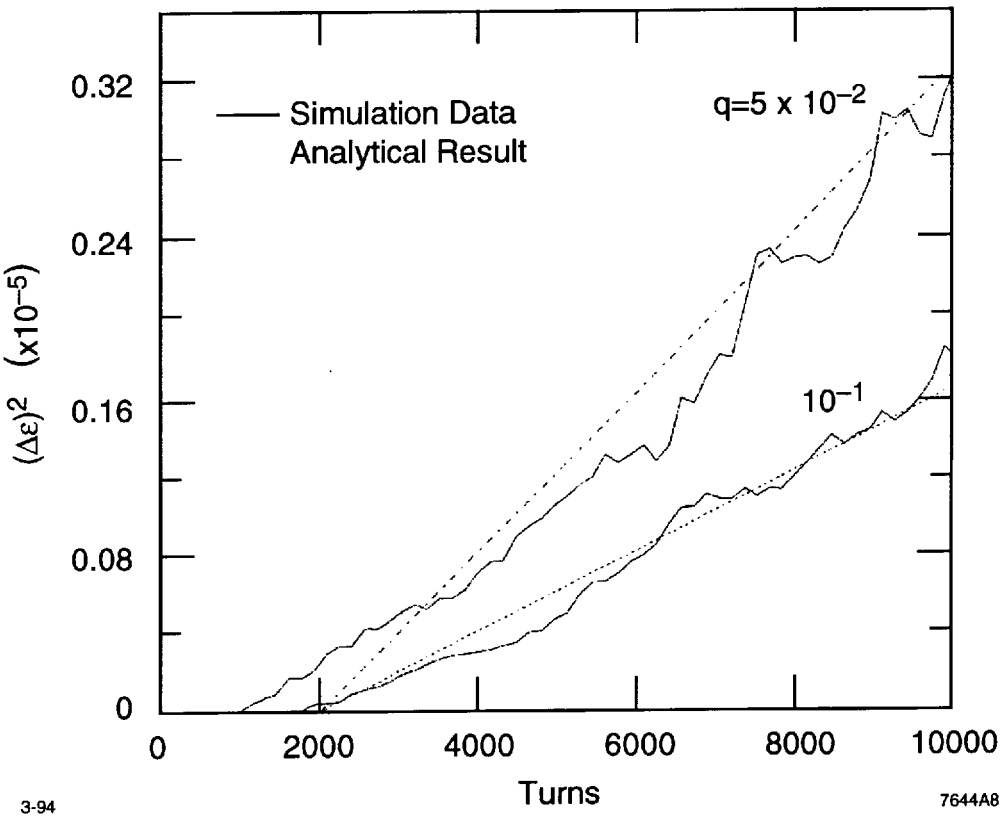
0.32
0.24
0.16
0.08
0
$(\Delta\varepsilon)^2$ $(x10^{-5})$
Simulation Data
Analytical Result
$q=5 \times 10^{-2}$
10^{-1}
0
2000
4000
6000
8000
10000
Turns
3-94
7644A8

Figure 8:

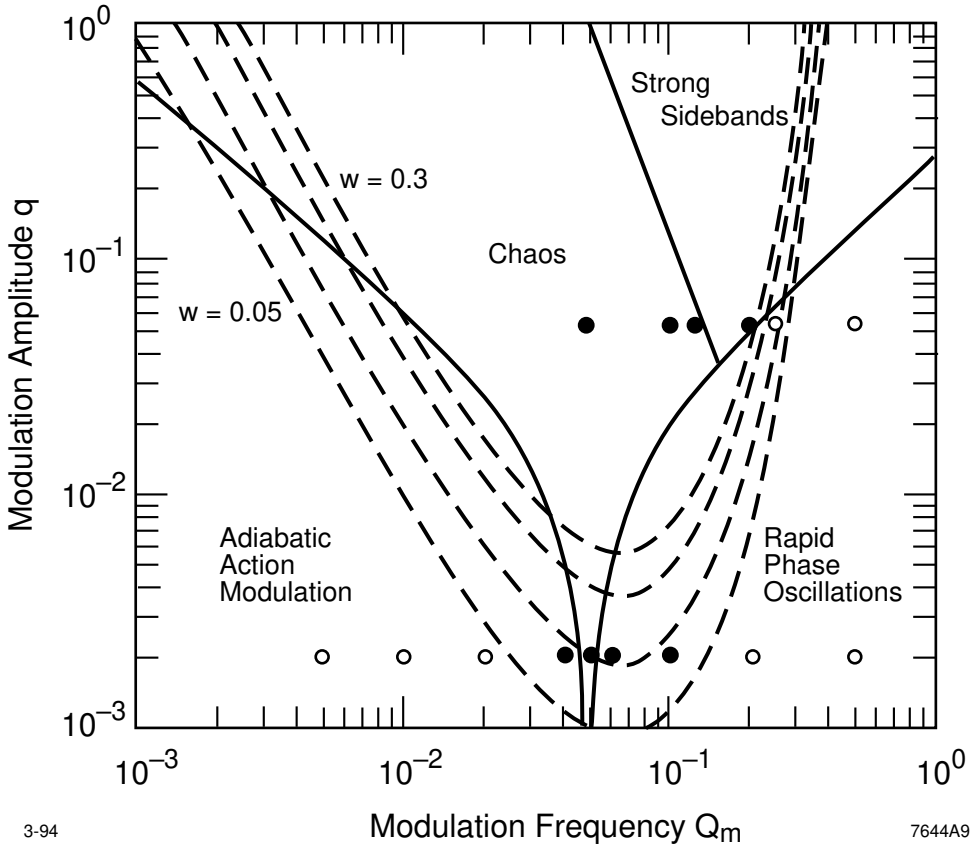
Strong
Sidebands
w = 0.3
Chaos
w = 0.05
Adiabatic
Action
Modulation
Rapid
Phase
Oscillations
Modulation Amplitude q
Modulation Frequency Qm
3-94
7644A9

Figure 9:

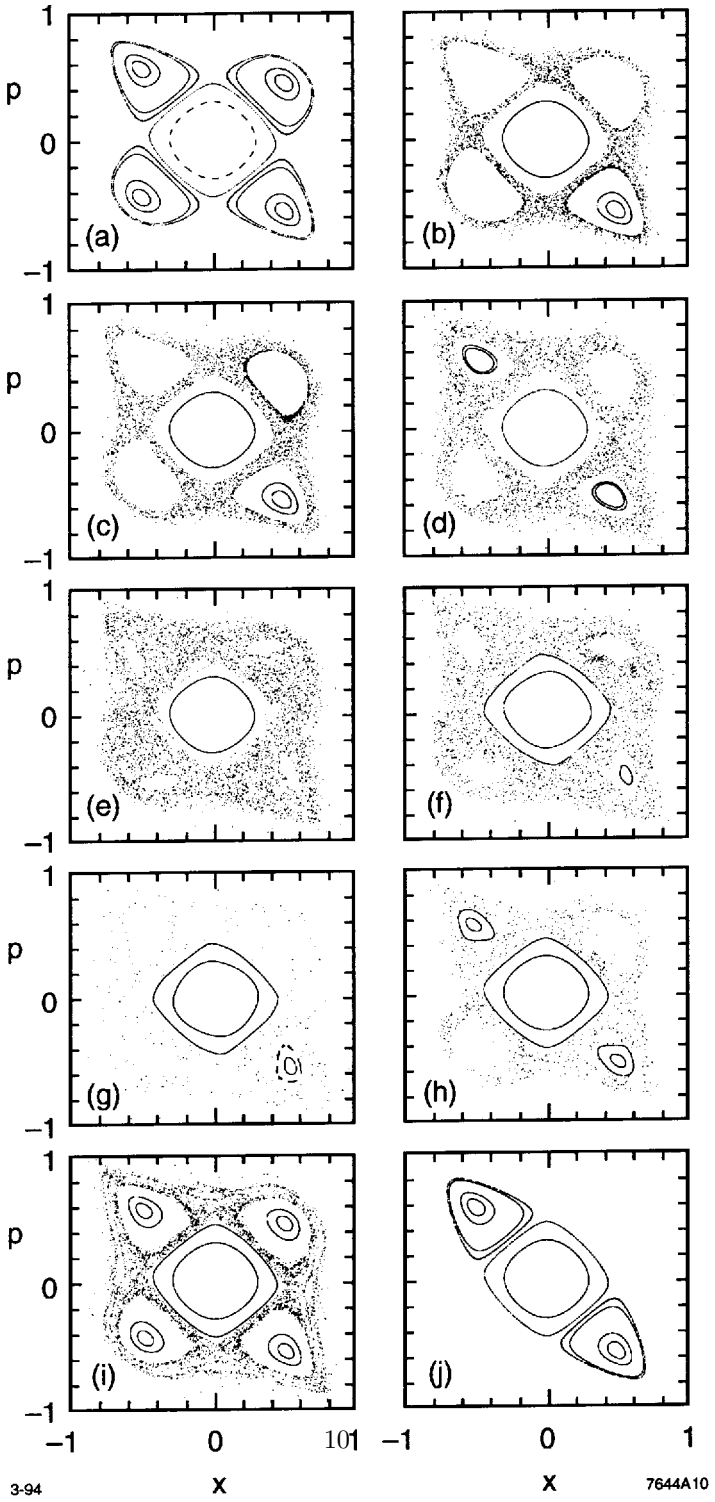

Figure 10:

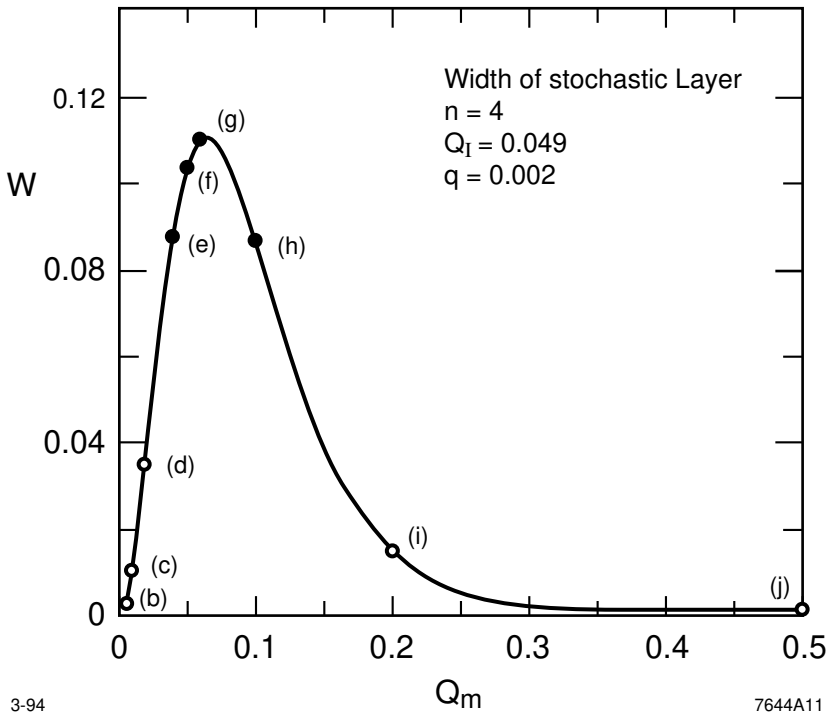
Width of stochastic Layer
n = 4
Q_I = 0.049
q = 0.002
W
0.12
0.08
0.04
0
0
0.1
0.2
0.3
0.4
0.5
Q_m
(b)
(c)
(d)
(e)
(f)
(g)
(h)
(i)
(j)
3-94
7644A11

Figure 11:

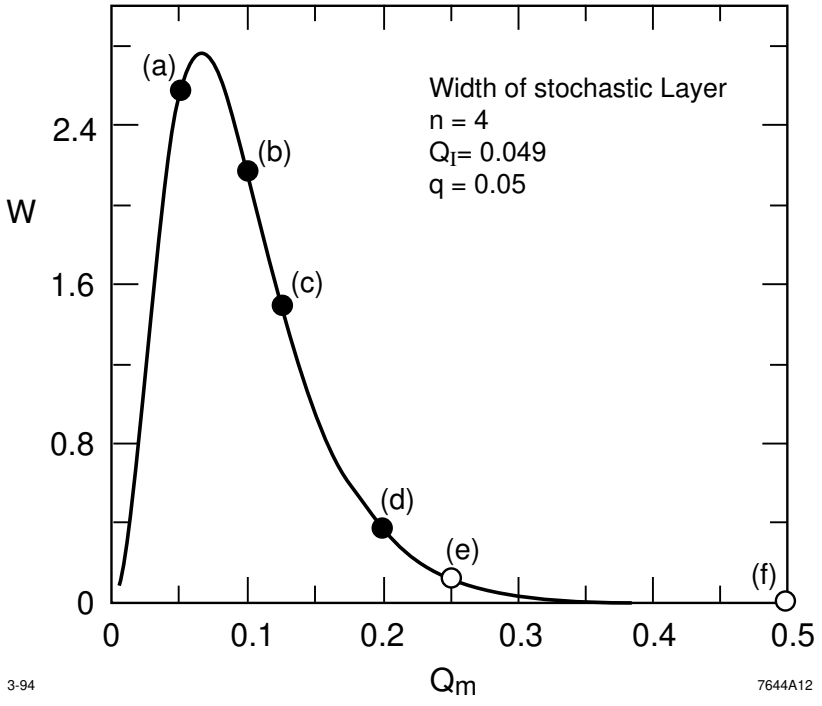
Width of stochastic Layer
n = 4
Q_I= 0.049
q = 0.05
(a)
(b)
(c)
(d)
(e)
(f)
W
2.4
1.6
0.8
0
0
0.1
0.2
0.3
0.4
0.5
Q_m
3-94
7644A12

Figure 12:

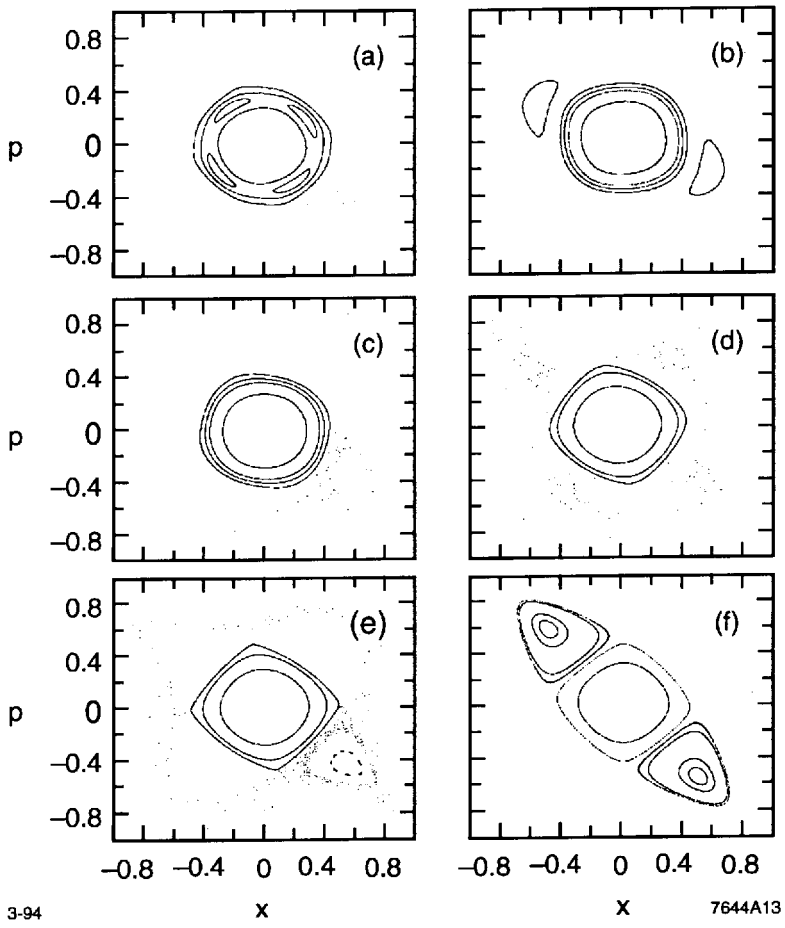

Figure 13:

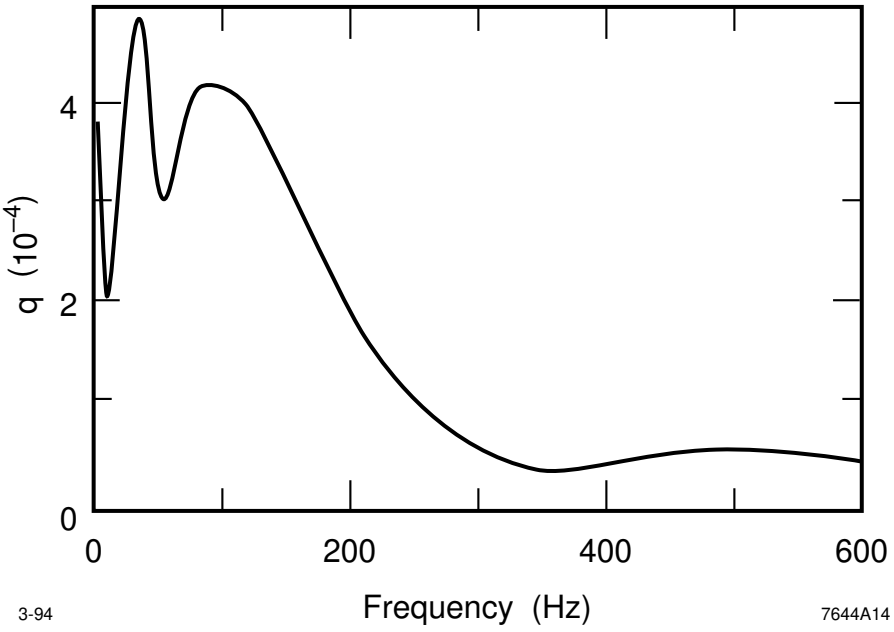

Figure 14:

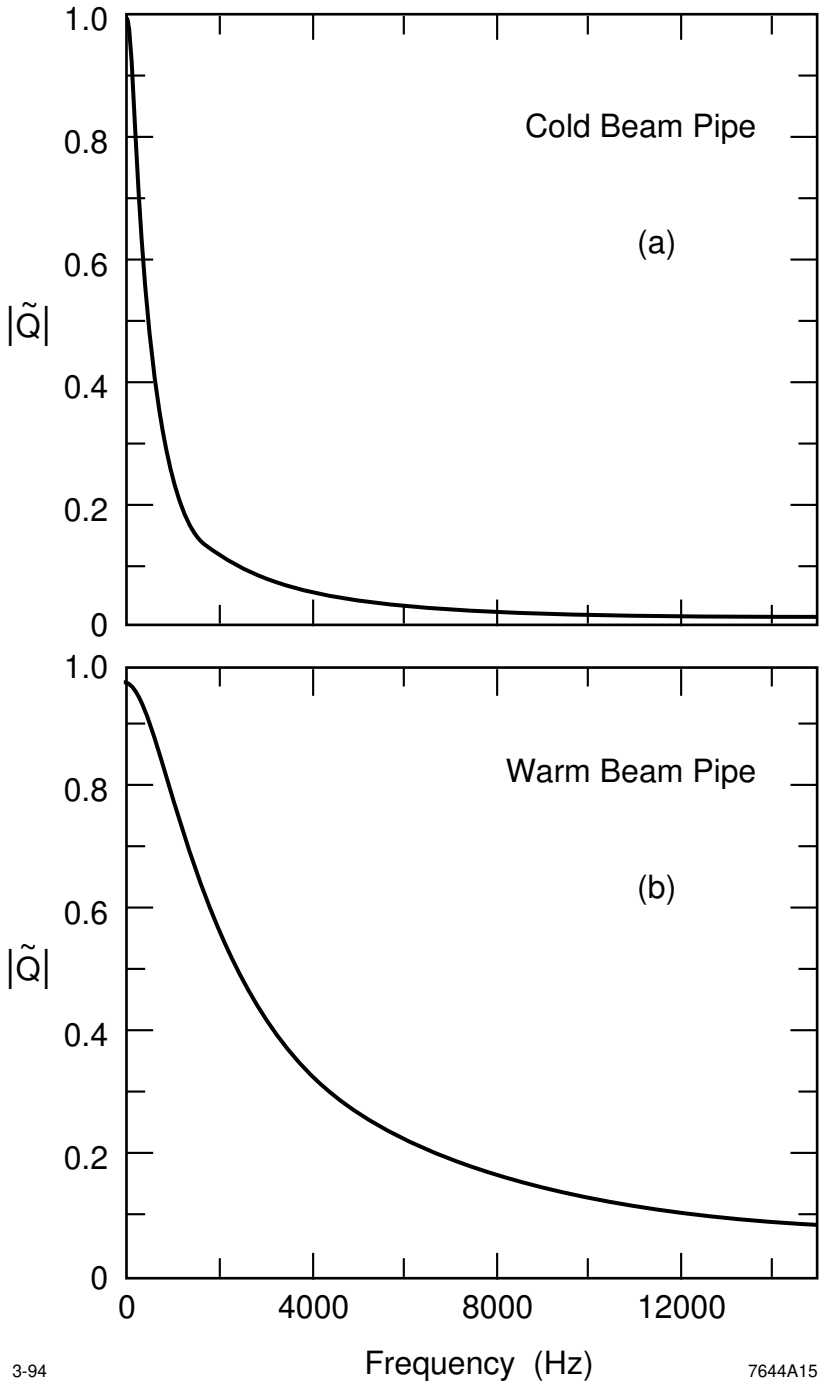
1.0
0.8
0.6
0.4
0.2
0
|Q̃|
Cold Beam Pipe
(a)
1.0
0.8
0.6
0.4
0.2
0
|Q̃|
Warm Beam Pipe
(b)
0
4000
8000
12000
Frequency (Hz)
3-94
7644A15

Figure 15:

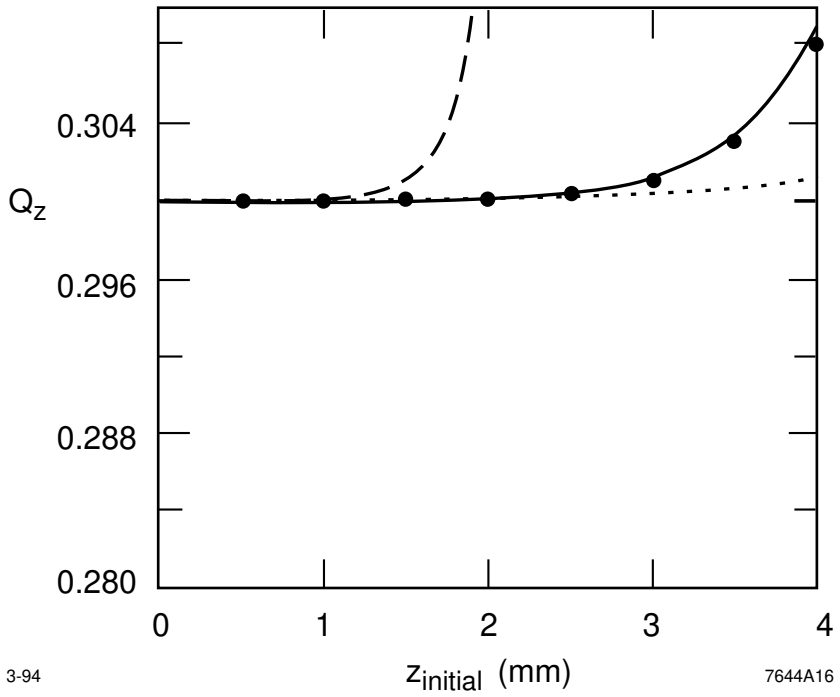

Figure 16:

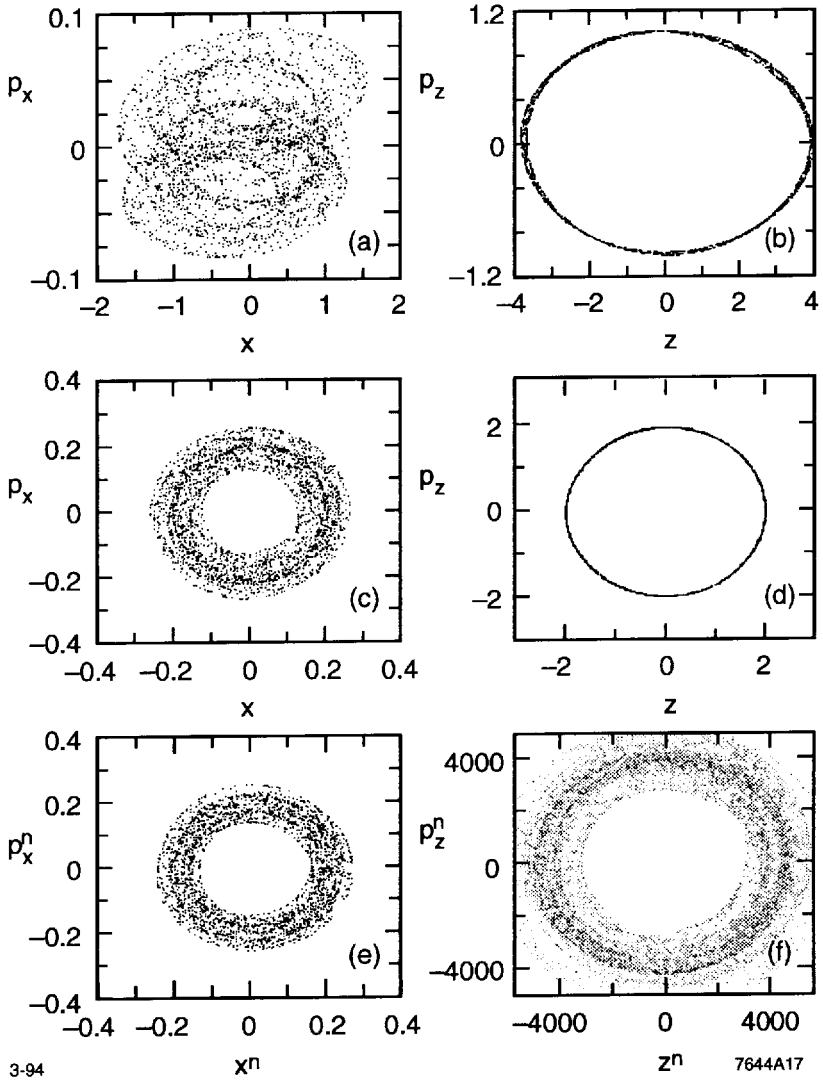
0.1
p_x
0
−0.1
−2
−1
0
1
2
x
(a)
1.2
p_z
0
−1.2
−4
−2
0
2
4
z
(b)
0.4
0.2
p_x
0
−0.2
−0.4
−0.4
−0.2
0
0.2
0.4
x
(c)
2
p_z
0
−2
−2
0
2
z
(d)
0.4
0.2
p_x^n
0
−0.2
−0.4
−0.4
−0.2
0
0.2
0.4
x^n
(e)
4000
p_z^n
0
−4000
−4000
0
4000
z^n
(f)
3-94
7644A17

Figure 17:

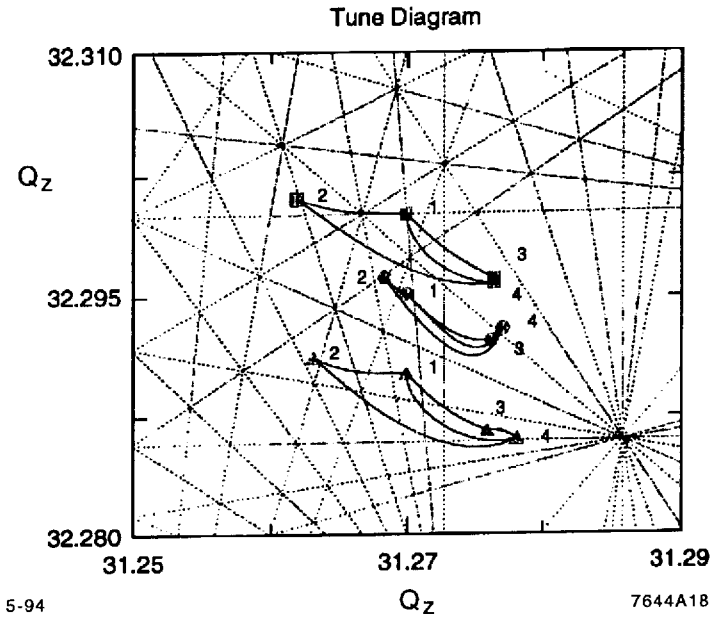
Tune Diagram
32.310
32.295
32.280
Q_z
31.25
31.27
31.29
Q_z
5-94
7644A18

Figure 18:

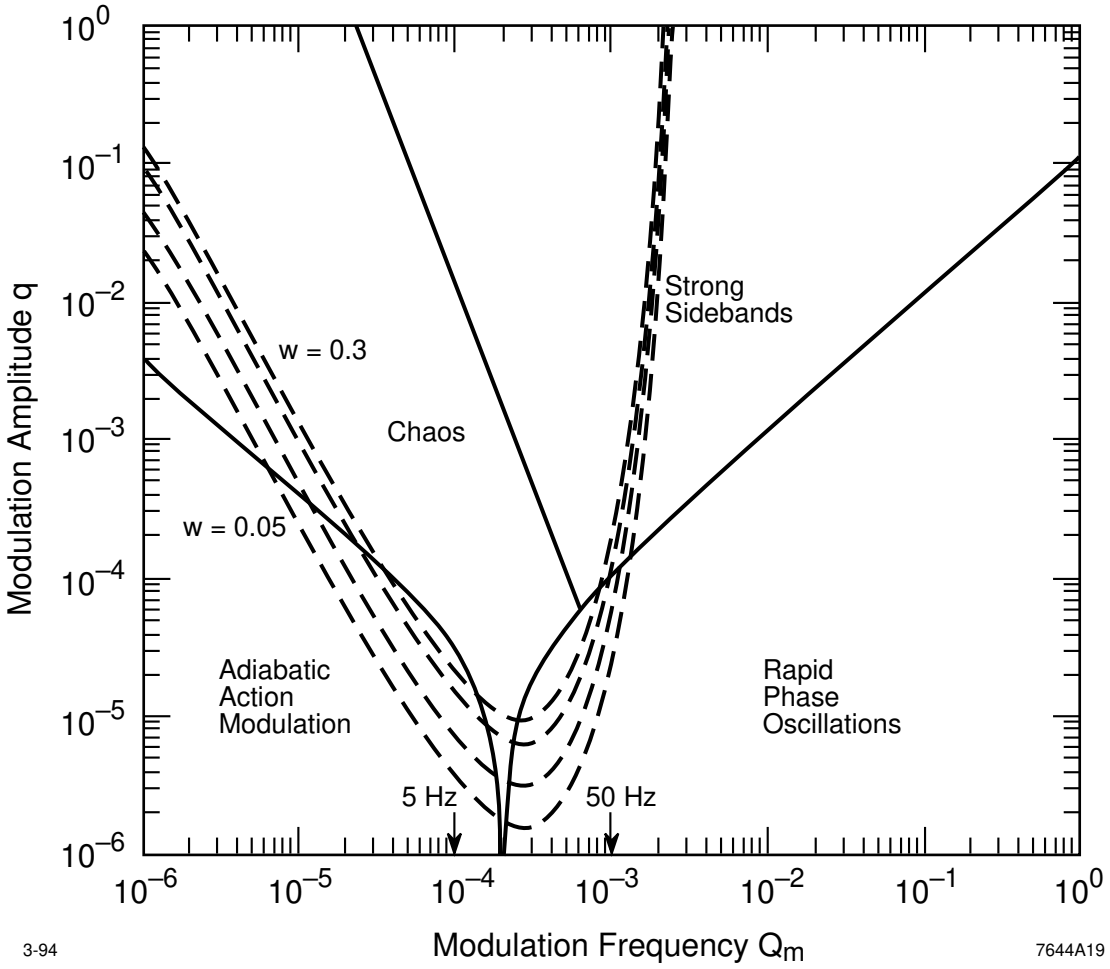
Modulation Amplitude q
Modulation Frequency Q_m
10^0
10^{-1}
10^{-2}
10^{-3}
10^{-4}
10^{-5}
10^{-6}
10^{-6}
10^{-5}
10^{-4}
10^{-3}
10^{-2}
10^{-1}
10^0
w = 0.3
w = 0.05
Chaos
Strong
Sidebands
Adiabatic
Action
Modulation
Rapid
Phase
Oscillations
5 Hz
50 Hz
3-94
7644A19

Figure 19:

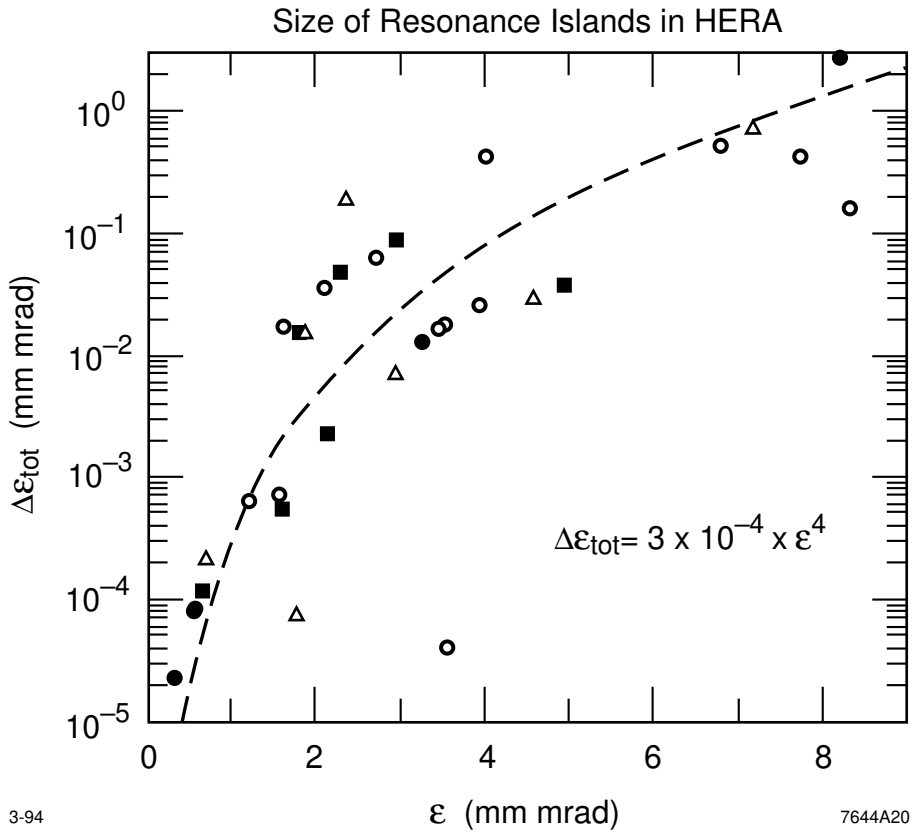
Size of Resonance Islands in HERA
$\Delta\varepsilon_{tot}$ (mm mrad)
ε (mm mrad)
$\Delta\varepsilon_{tot}= 3 \times 10^{-4} \times \varepsilon^4$
3-94
7644A20

Figure 20:

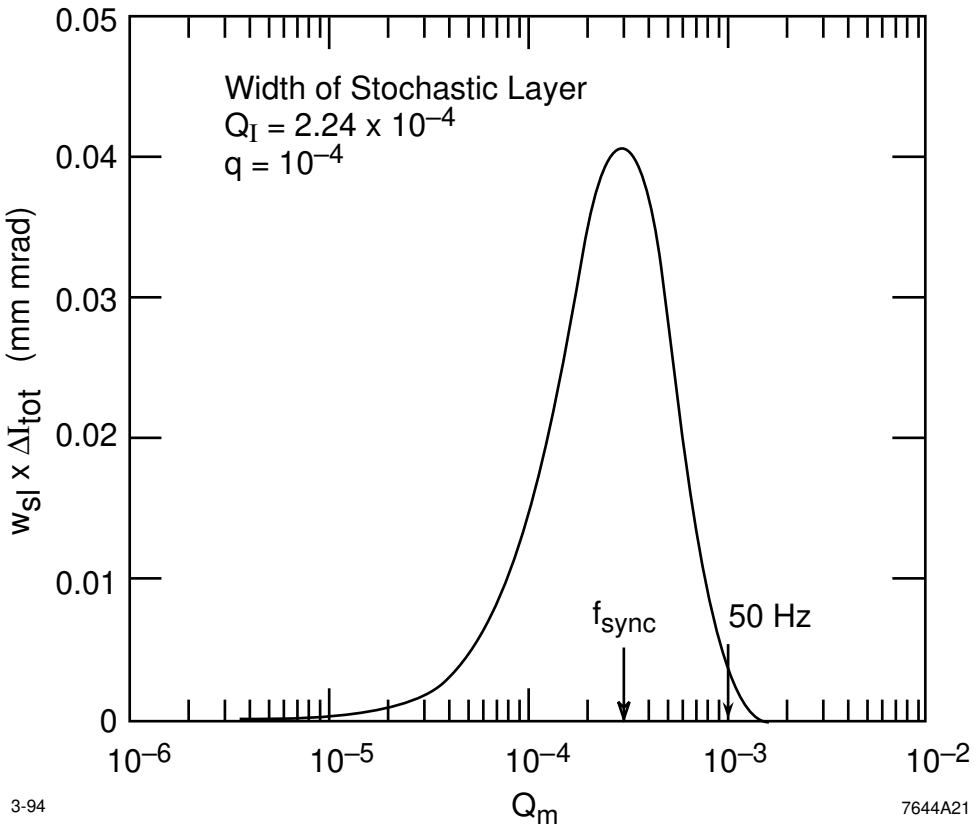
Width of Stochastic Layer
$Q_I = 2.24 \times 10^{-4}$
$q = 10^{-4}$
$w_{sl} \times \Delta I_{tot}$ (mm mrad)
0.05
0.04
0.03
0.02
0.01
0
f_{sync}
50 Hz
10^{-6}
10^{-5}
10^{-4}
10^{-3}
10^{-2}
Q_m
3-94
7644A21

Figure 21:

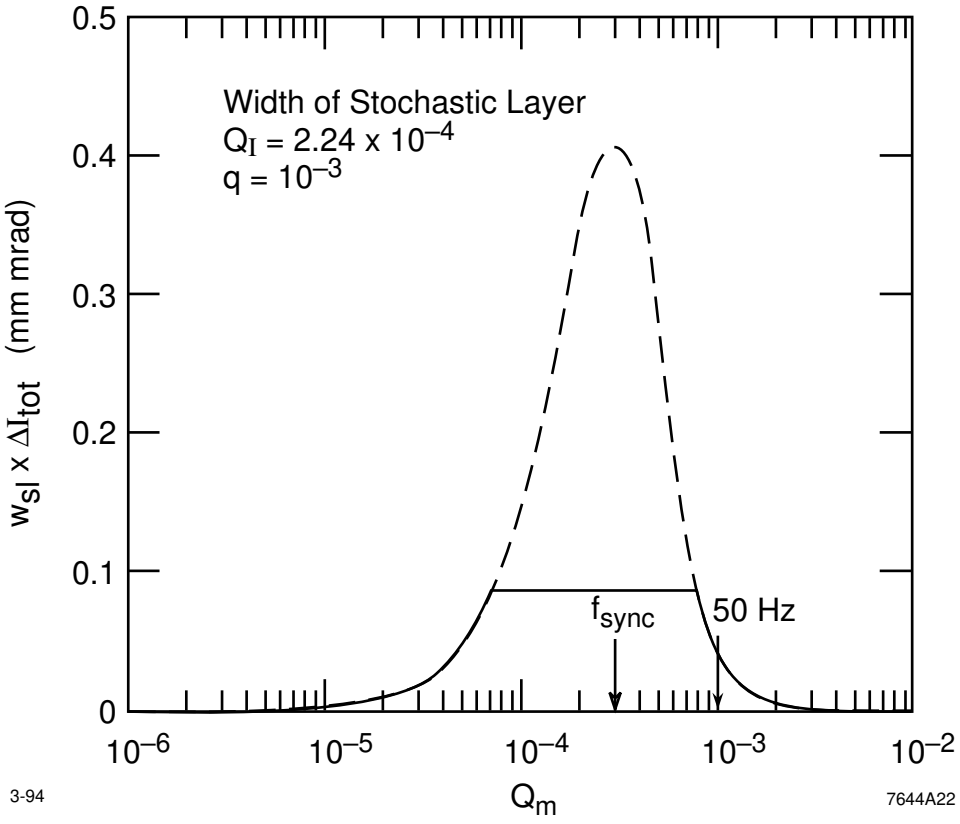
Width of Stochastic Layer
$Q_I = 2.24 \times 10^{-4}$
$q = 10^{-3}$
$w_{sl} \times \Delta I_{tot}$ (mm mrad)
0.5
0.4
0.3
0.2
0.1
0
f_{sync}
50 Hz
10^{-6}
10^{-5}
10^{-4}
10^{-3}
10^{-2}
Q_m
3-94
7644A22

Figure 22:

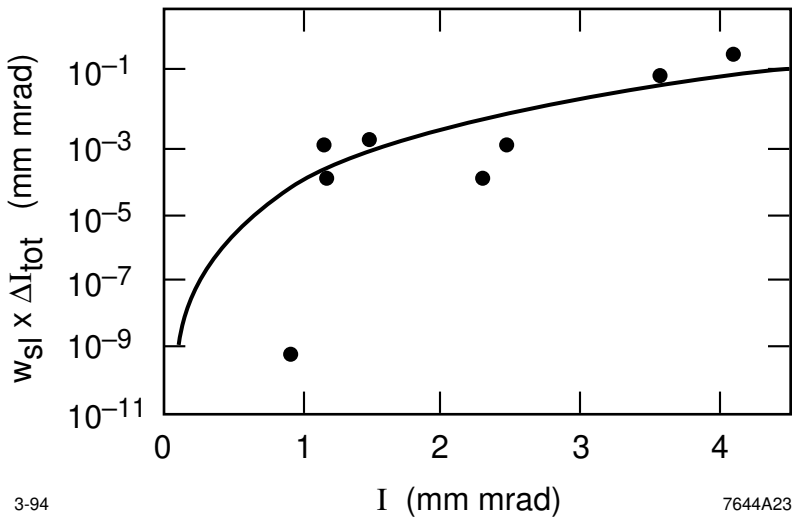
$w_{SI} \times \Delta I_{tot}$ (mm mrad)
10^{-1}
10^{-3}
10^{-5}
10^{-7}
10^{-9}
10^{-11}
0
1
2
3
4
I (mm mrad)
3-94
7644A23

Figure 23:

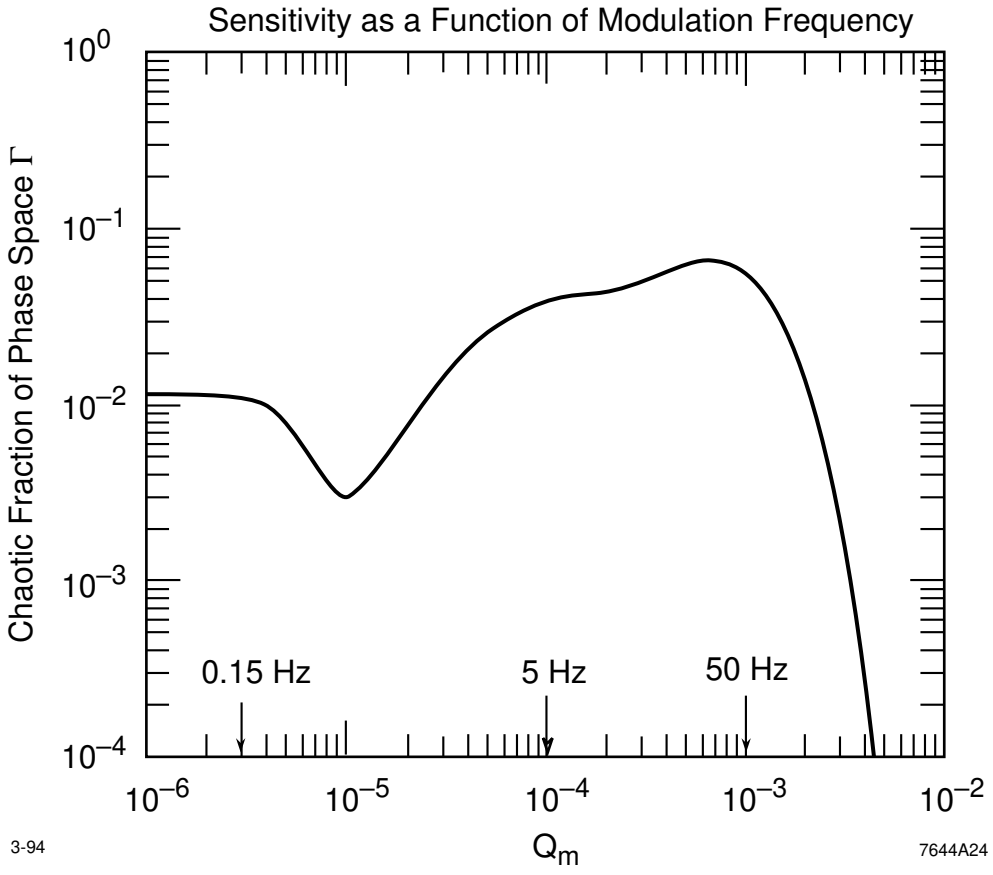
Sensitivity as a Function of Modulation Frequency
Chaotic Fraction of Phase Space Γ
10^0
10^{-1}
10^{-2}
10^{-3}
10^{-4}
0.15 Hz
5 Hz
50 Hz
10^{-6}
10^{-5}
10^{-4}
10^{-3}
10^{-2}
Q_m
3-94
7644A24

Figure 24:

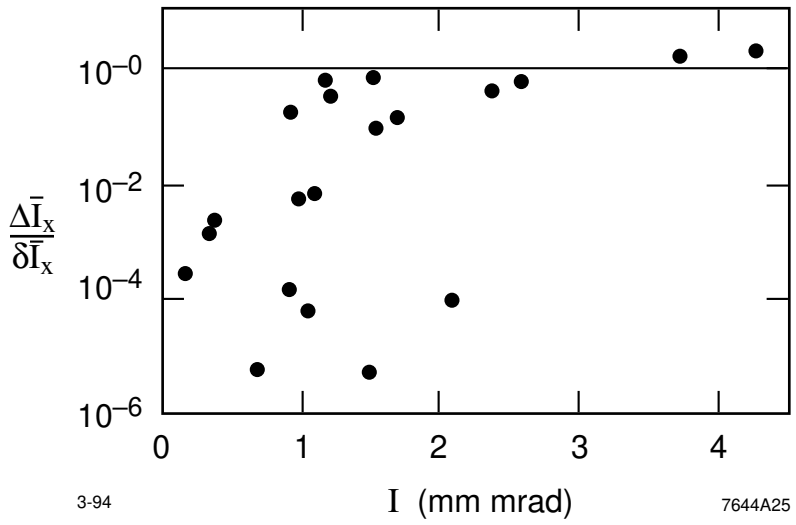
10^{-0}
10^{-2}
10^{-4}
10^{-6}
$\frac{\Delta \bar{I}_x}{\delta \bar{I}_x}$
0
1
2
3
4
I (mm mrad)
3-94
7644A25

Figure 25:

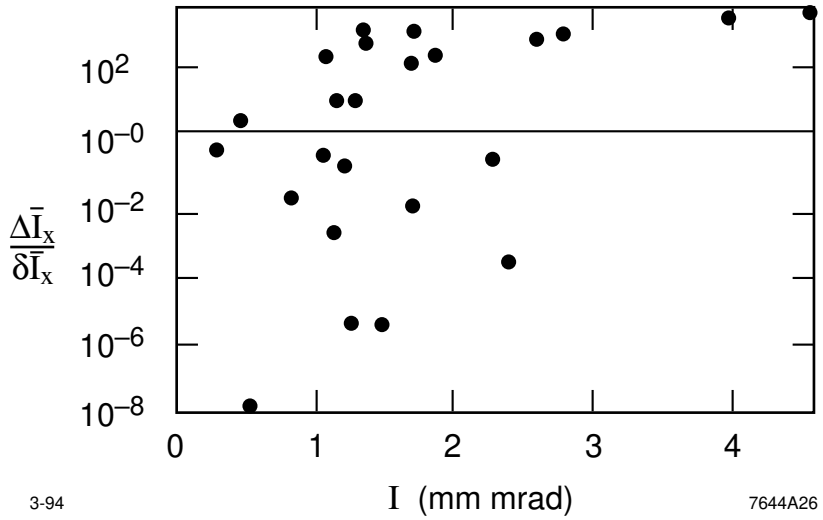

Figure 26:

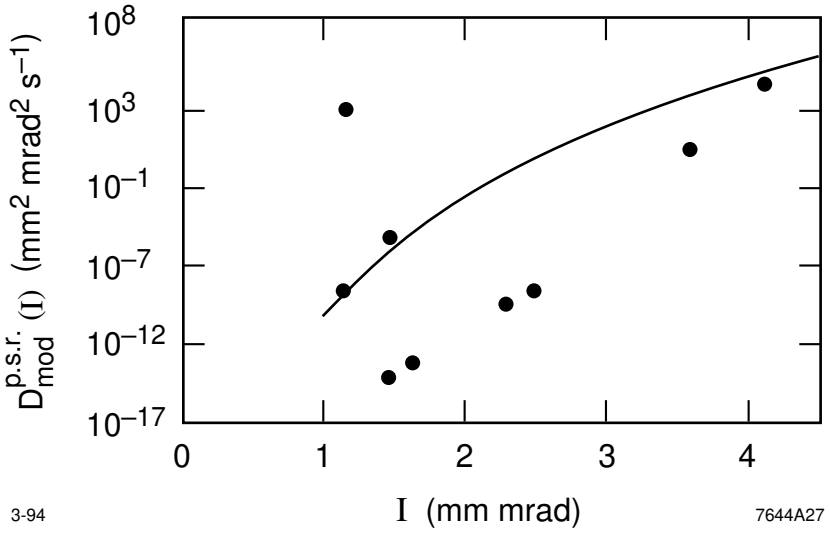

Figure 27:

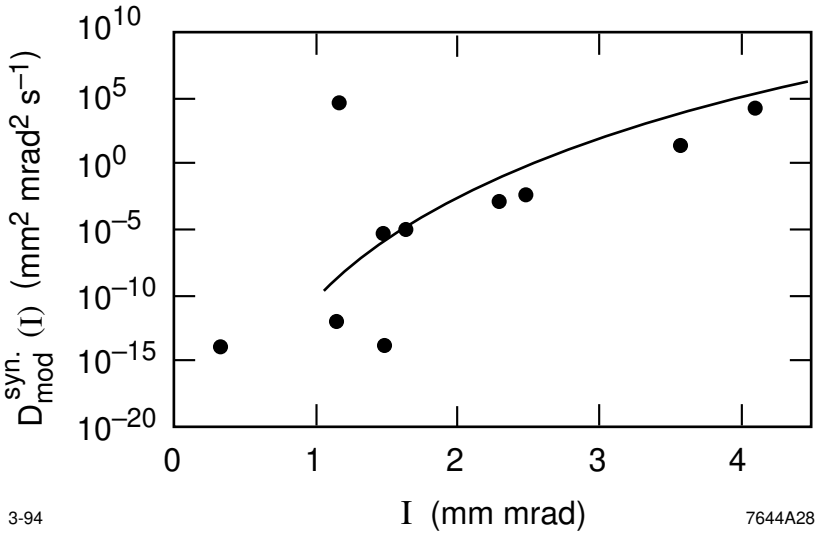

Figure 28:

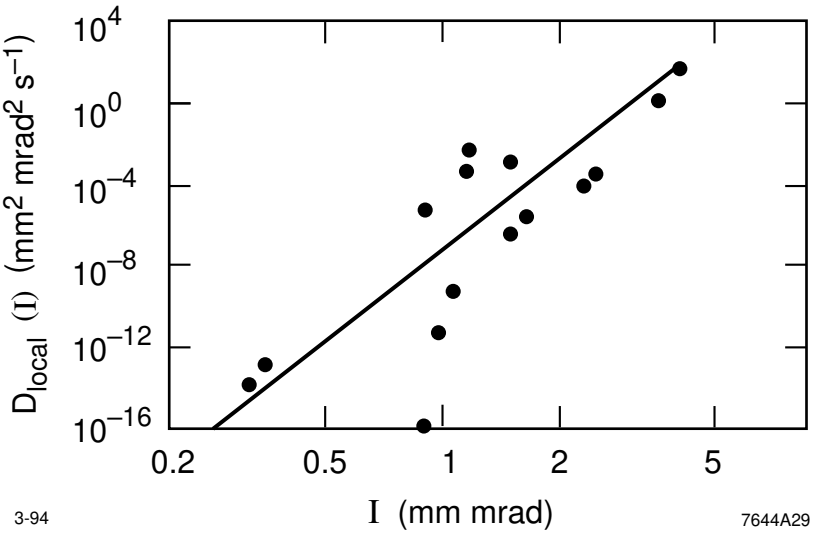

Figure 29:

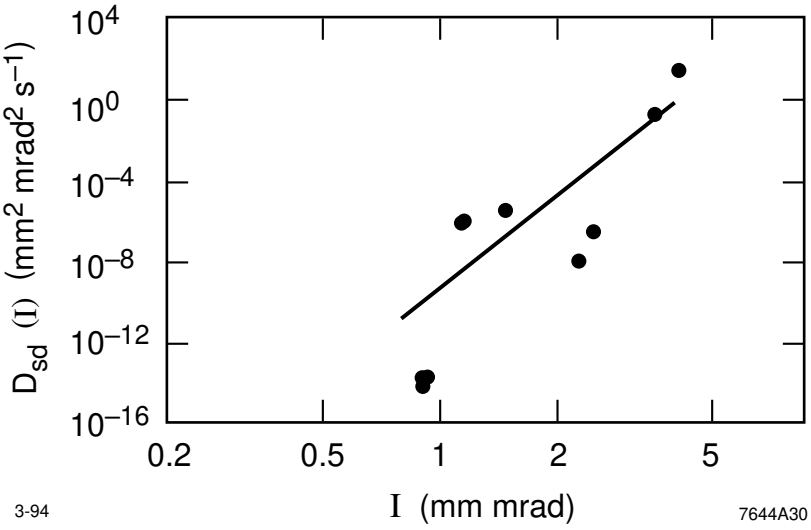
10^4
10^0
10^{-4}
10^{-8}
10^{-12}
10^{-16}
D_{sd} (I) (mm^2 $mrad^2$ s^{-1})
0.2
0.5
1
2
5
I (mm mrad)
3-94
7644A30

Figure 30:

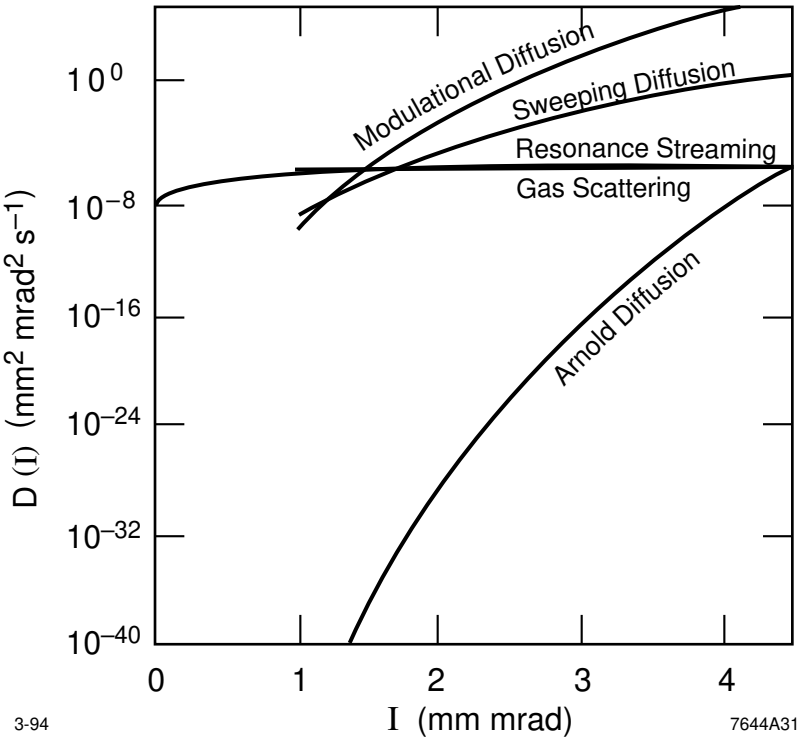
Modulational Diffusion
Sweeping Diffusion
Resonance Streaming
Gas Scattering
Arnold Diffusion
10^{0}
10^{-8}
10^{-16}
10^{-24}
10^{-32}
10^{-40}
D (I) (mm^2 mrad^2 s^{-1})
0
1
2
3
4
I (mm mrad)
3-94
7644A31

Figure 31:

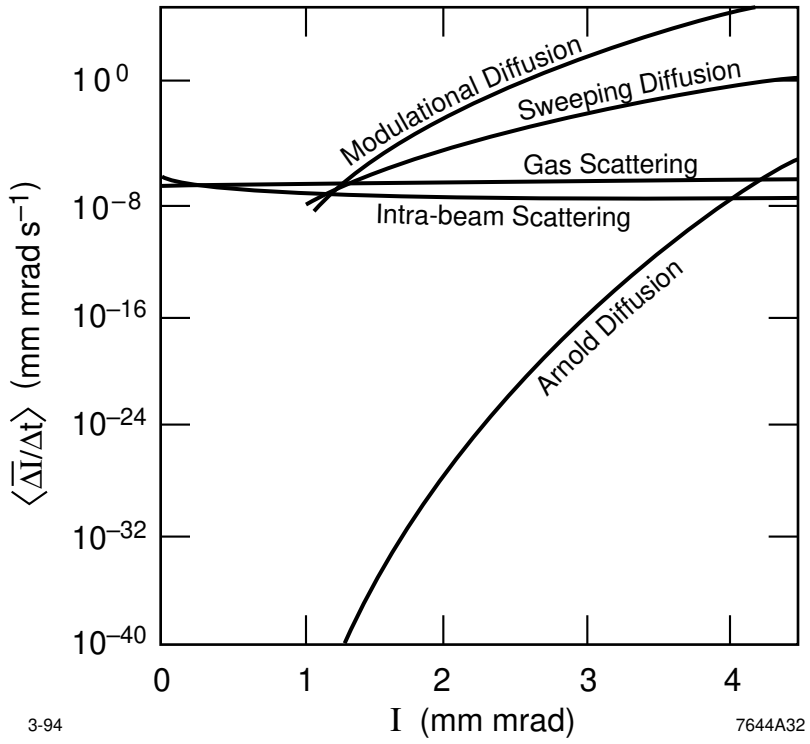
Modulational Diffusion
Sweeping Diffusion
Gas Scattering
Intra-beam Scattering
Arnold Diffusion
10^{0}
10^{-8}
10^{-16}
10^{-24}
10^{-32}
10^{-40}
$\langle \overline{\Delta I/\Delta t} \rangle$ (mm mrad s^{-1})
0
1
2
3
4
I (mm mrad)
3-94
7644A32

Figure 32: